

Bree's interaction diagram of beams with considering creep and ductile damage

A. Nayebi[†]

Department of Mechanical Engineering, School of Engineering, Shiraz University, Shiraz, Iran

(Received August 31, 2007, Accepted October 12, 2008)

Abstract. The beams components subjected to the loading such as axial, bending and cyclic thermal loads were studied in this research. The used constitutive equations are those of elasto-plasticity coupled to ductile and/or creep damage. The nonlinear kinematic hardening behavior was considered in elasto-plasticity modeling. The unified damage law proposed for ductile failure and fatigue by the author of Sermage *et al.* (2000) and Kachanov's creep damage model applied to cyclic creep and low cycle fatigue of beams. Based on the results of the analysis, the shakedown limit loads were determined through the calculation of the residual strains developed in the beam analysis. The iterative technique determines the shakedown limit load in an iterative manner by performing a series of full coupled elastic-plastic and continuum damage cyclic loading modeling. The maximum load carrying capacity of the beam can withstand, were determined and imposed on the Bree's interaction diagram. Comparison between the shakedown diagrams generated by or without creep and/or ductile damage for the loading patterns was presented.

Keywords: Bree's diagram; ductile damage; creep damage; cyclic loading; nonlinear kinematic hardening.

1. Introduction

Components of power plants such as rotors, castings and components of turbines, components of chemical plants and ... have to face the combination of highly damaging processes due to the operating temperatures and the numbers of start-up and shut-down. These processes involve creep, thermal fatigue and ductile plastic damage. The determination of the plastic damage behavior of a component is already complicated business, but it becomes much more complicated when creep damage occurs. In the past, some models have been applied to model cyclic loading of beams Mahbadi, Gowhari, and Eslami (2004), Eslami and Mahbadi (2002) but they are restricted to linear or non linear kinematic hardening.

The degradation phenomenon (microcracks, microcavities, nucleation and coalescence, decohesions, grain boundary cracks, and cleavage in regions of high stress concentration) are better described by theories of plasticity and continuum damage mechanics. Ductile materials usually failed as the result of the nucleation, growth, and the coalescence of the microdamage. Experimental

[†] Professor, E-mail: nayebi@shirazu.ac.ir

observations indicate that the accumulation of the microdamage has a tendency to form macroscopically localized damage, which is a precursor to failure. This progressive physical process of degradation of the material's mechanical properties up to complete failure is commonly referred to as the damage. Variation of damage morphologies has been described in the literature as: creep damage, low cycle fatigue, high cycle fatigue, and brittle damage.

The creep–ductile damage interaction models have not extensively applied to engineering problems because of high degree of complexity. For example some of the existing models are: (i) the linear interaction rule Taira (1962), (ii) the Coffin model (1976), where the frequency is introduced in the Manson–Coffin relation (1954), (iii) the strain range partitioning Manson (1971) and (iv) the creep–fatigue damage model Lemaitre and Chaboche (1974) where the creep damage and fatigue damage are both considered as non-linear functions of the three-dimensional state of stress Sermage *et al.* (2000). This model gives good results, but the identification of the nine material parameters is not an easy task!

Sermage *et al.* (2000) showed that a much simpler law of damage evolution which is based on thermodynamics and first proposed for ductile damage Lemaitre (1985) is able to represent creep–fatigue interaction. The mentioned models need only four material-dependent parameters to be identified. Successfully, this model has been applied to low-cycle Lemaitre and Desmorat (2005) and high-cycle fatigue damage in a two-scale model Desmorat, Kane, Seyedi, and Sermage (2007).

Very limited works have been published on damage related to thermo-mechanical loading of beam problems. Krajcinovic (1979) applied the damage concept for beam bending problems for the first time. Also he defined the isotropic damage variable by means of a parameter called the damage modulus, which is related to the fracture stress. Ultimate moment carrying capacities and the shift of the neutral axis were computed for concrete beams, using this damage model. Shi and Voyiadjis (1993) have illustrated the use of Lemaitre's damage model for beam and plate bending problems. Chandrakanth and Pandey (1995) have developed an exponential damage model for low carbon steel and used it to analyze notched beams to predict their fracture initiation loads. The predicted fracture loads have been compared with experimental results.

When the cyclic load lies between the first yield and plastic collapse loads, three types of elastic–plastic behaviour may occur; Elastic Shakedown, Plastic Shakedown (Alternating Plasticity), or Ratchetting. The limit loads between shakedown and ratcheting states are known as shakedown limit loads and Shakedown analysis of elastic–plastic structures aims to obtain the shakedown state for a given domain of variable loads.

The boundaries between these states for different structures can be shown in an interaction diagram (Bree's diagram). The interaction diagram obtained by Bree (1967) and developed by O'Donnell and Porowski (1981), and it is a part of the ASME III NH high temperature code (1998) now. Bree (1967) considered a steady-state pressure load (primary membrane stress) and a linear through the wall temperature distribution (secondary bending thermal stress) that is applied and then removed. Then the elastic, shakedown and ratchetting regimes were obtained. This diagram shows the safety regions in the constant primary plus cyclic secondary stresses which is an important tool in design by analysis. It is a need to obtain the Bree's diagram for different structures.

The aim of this research is to investigate the cyclic loading of beams under different types of loading such as thermal, mechanical and their combination. The elastic–plastic and creep damage analysis was performed to study the behaviour of the beam structures under load and deformation controlled conditions. Kinematic hardening theory was used to model the plastic behaviour of the beams. An iterative method is proposed to analyze the beam under the cyclic thermal and

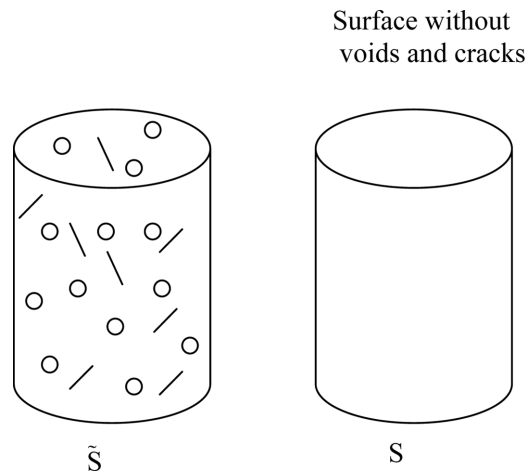


Fig. 1 Definition of the surface (S) and the effective resistant surface (\tilde{S})

mechanical loads. Numerical examples illustrate the influence of material damage in comparison with confirmed results on undamaged structures.

2. Constitutive behaviour relations

2.1 Continuum damage mechanics

According to the applied theory of damage mechanics, microscopic change in a material element of surface S causes macroscopic change of the element to its damaged state \tilde{S} due to service condition (Fig. 1), from which the isotropic damage variable D is defined as Lemaitre (1992)

$$D = \frac{S - \tilde{S}}{S} \quad (1)$$

D may be considered as an internal state variable characterizing the irreversible deterioration of a material in the thermodynamic sense. Following this theory, the behavior of a damaged material can be represented by the constitutive equations of the virgin material where the usual stress tensor σ is replaced by the effective stress $\tilde{\sigma}$ defined by

$$\tilde{\sigma} = \frac{\sigma}{1 - D} \quad (2)$$

where the value $D=0$ corresponds to the undamaged state, $D \in (0, D_c)$ corresponds to a partly damaged state and $D=D_c$ defines the element state rupture by interatomic decoherence ($D_c \in [0, 1]$). In the sequel, superposed tilda indicates quantities related to the damaged state of the material.

2.2 Plastic ductile damage

Observations and experiments indicate that the plastic ductile damage is governed by the plastic strain which is introduced through the plastic multiplier, λ , as

$$\dot{D} = \lambda \frac{\partial F_D}{\partial Y} \quad \text{if } \varepsilon_p > \varepsilon_p^D \quad (3)$$

with λ calculated from the constitutive equations of plasticity coupled with the damage deduced from the dissipative potential function and Y is the associate variable of the damage rate, \dot{D} . ε_p^D is the plastic damage threshold strain. Experimental results show that F_D must be a nonlinear function of Y Lemaître (1992)

$$F_D = \frac{Q}{(q+1)(1-D)} \left(\frac{Y}{Q} \right)^{q+1} \quad (4)$$

from which Eq. (3)

$$\dot{D} = \left(\frac{Y}{Q} \right)^q \dot{p} \quad (5)$$

Q and q are two material parameters, $\dot{p} = (2/3 \varepsilon_p : \dot{\varepsilon}_p)^{1/2}$ is the accumulated plastic strain rate (in which: indicates the product of two tensors) and according to Lemaître and Desmorat (2005)

$$\begin{cases} Y = \frac{\tilde{\sigma}_{eq}^2 R_v}{2E} \\ R_v = \frac{2}{3}(1+\nu) + 3(1-2\nu) \left(\frac{\sigma_H}{\sigma_{eq}} \right)^2 \end{cases} \quad (6)$$

where $\sigma_{eq} = (3/2 \sigma' : \sigma')^{1/2}$ is the von Mises equivalent stress ($\sigma' = \sigma - \sigma_H \delta_{ij}$) and $\sigma_H = 1/3 \text{tr}(\sigma)$ the hydrostatic stress (δ_{ij} is the Kronecker unit tensor). Defining the critical value of the damage, D_c , at mesocrack initiation and the plastic strain at the rupture ε_p^R

$$D_c = \left(\frac{\sigma_u^2}{2EQ} \right)^q (\varepsilon_p^R - \varepsilon_p^D) \quad (7)$$

the damage law (Eq. (5)) reduces to Chaboche and Lemaître (1990)

$$\dot{D} = \frac{D_c}{\varepsilon_p^R - \varepsilon_p^D} \left[\frac{2}{3}(1+\nu) + 3(1-2\nu) \left(\frac{\sigma_H}{\sigma_{eq}} \right)^2 \right] \dot{p} \quad (8)$$

and by the integration

$$\dot{D} = \frac{D_c}{\varepsilon_p^R - \varepsilon_p^D} \left\langle \left[\frac{2}{3}(1+\nu) + 3(1-2\nu) \left(\frac{\sigma_H}{\sigma_{eq}} \right)^2 \right] p - \varepsilon_p^D \right\rangle \quad (9)$$

with $\langle x \rangle = x$ if $x > 0$, and $\langle x \rangle = 0$ if $x \leq 0$,

This model depends upon material constants ε_p^D (damage threshold strains), ε_p^R (strain at fracture) and D_c (critical value of damage parameter at fracture) for damage properties and Poisson's ratio ν .

In one dimensional problem, Eq. (8) reduces to

$$\dot{D} = \frac{D_c}{\varepsilon_p^R - \varepsilon_p^D} \dot{p} \quad (10)$$

So the damage parameter is related to the accumulated plastic strain and it is coupled with the plasticity. Assuming the Von-Mises yield criteria, the elastic domain can be rewritten by replacing

the stress by the effective stress, $\tilde{\sigma}$, as

$$f(\tilde{\sigma}, X) = f\left(\frac{\sigma}{1-D}, X\right) \quad (11)$$

where X is the coordinates of the yield surface center.

2.3 Creep damage

Both stress relaxation response and load controlled creep can be described using a primary modified continuum damage mechanics model of the Rabotnov-Kachanov type (2005). The model can be derived from potential written as Lemaitre (1984)

$$F_D = \frac{1}{\frac{r_D}{2} + 1} \left(\frac{A_D}{2E}\right) \left(-Y \frac{2E}{A^2}\right)^{1+r_D/2} \quad (12)$$

from which, the coupled equation of the general form

$$\dot{D} = \left[\frac{\sigma_{eq}}{A_D(1-D)} \right]^{r_D} \quad (13)$$

where A_D and r_D are material parameters. Their model can be obtained from Eq. (5) by considering a Norton viscosity law.

The stress triaxiality has important effects such as the progressive reduction of material ductility with increasing stress triaxiality factor (σ_H/σ_{eq}) Lemaitre (1992). Although this effect was not taken into account in the Kachanov's model, but the considered loadings in this research, lead to a 1-D beam problem, and so the triaxiality ration ($\sigma_H/\sigma_{eq}=1/3$) is constant and does not influence the obtained results.

Eq. (13) may be integrated numerically over any loading history to give the evolution of strain and damage until failure. Under conditions of displacement control, total relaxation of the initial stress occurs at infinite time. Under general thermo-mechanical loading conditions, there are contributions from primary and secondary stresses. Redistribution and relaxation of combined stress will tend, generally, to a non-zero value of stress, which is achieved within a finite time.

2.4 Non linear kinematic hardening

Constitutive model for cyclic plasticity was used in ductile plastic deformation. The non-linear hardening model has a yield condition with internal state variables and utilizes the normality hypothesis with the associated flow rule:

$$f(\tilde{\sigma}, X) = \{(\tilde{\sigma}' - X') : (\tilde{\sigma}' - X')\}^{1/2} = \{(\tilde{\sigma}'_{ij} - X'_{ij}) (\tilde{\sigma}'_{ij} - X'_{ij})\}^{1/2} - \sigma_y \quad (14)$$

$$d\epsilon_{ij}^p = \frac{3}{2} \frac{d\lambda}{1-D} \frac{(\tilde{\sigma}'_{ij} - X'_{ij})}{(\tilde{\sigma}'_{ij} - X'_{ij})_{eq}} \quad (15)$$

$$dX_{ij} = 2/3 C d\epsilon_{ij}^p (1-D) - \gamma X_{ij} d\lambda \quad (16)$$

where, $\tilde{\sigma}_{ij}$ and X_{ij} are the component of the effective stresses and the component of the back stress tensors, and $\tilde{\sigma}'_{ij}$ and X'_{ij} are the component of the effective stresses and the component pf the back

stress deviatoric tensors in the stress space, respectively. $d\lambda$ is the increment of the plastic multiplier calculated from the consistency condition:

$$df = \frac{\partial f}{\partial \sigma_{ij}} d\sigma_{ij} + \frac{\partial f}{\partial X_{ij}} dX_{ij} + \frac{\partial f}{\partial D} dD \quad (17)$$

By writing this consistency condition, the normality rule, the constitutive model and the yield function, the exact expression of $d\lambda$ can be obtained Lemaitre (1992)

$$d\lambda = \frac{3}{2} (\tilde{\sigma}'_{ij} - X_{ij}) d\sigma_{ij} / \left\{ (\tilde{\sigma}' - X)_{eq} (1 - D) \cdot \left[X_{\infty} \gamma - \frac{3(\tilde{\sigma}'_{ij} - X_{ij})}{2(\tilde{\sigma}' - X)_{eq}} \left(\gamma X_{ij} + \frac{\tilde{\sigma}'_{ij}}{1 - D} \frac{\partial F_D}{\partial Y} \right) \right] \right\} \quad (18)$$

where $X_{\infty} = \frac{2C}{3\gamma}$.

3. Elasto-plastic damage formulation of a beam

3.1 Elasto-plasticity coupled to ductile damage formulation

Consider a beam of isotropic material under the axial load P , bending moment M , and the transverse temperature distribution (Fig. 2). The total axial strain in the beam is

$$\varepsilon = \frac{\tilde{\sigma}}{E} + \varepsilon_p + \varepsilon^T = \frac{\sigma}{E} + \varepsilon_p + \alpha T \quad (19)$$

Where σ is the axial stress, ε_p is the axial plastic strain, T is the temperature distribution across the beam thickness, E is the modulus of elasticity, and α is the linear coefficient of thermal expansion. The dimensionless quantities are defined as

$$e = \frac{\varepsilon}{\varepsilon_y}, \quad s = \frac{\sigma}{\sigma_y}, \quad e^p = \frac{\varepsilon_p}{\varepsilon_y}, \quad \tau = \frac{\alpha T}{\varepsilon_y}, \quad \eta = \frac{y}{h}, \quad x = \frac{X}{\sigma_y}, \quad (20)$$

where $2h$ is the height of the beam cross section, ε_y is the initial yield strain, and σ_y is the initial yield stress. The dimensionless form of Eq. (19) is

$$e = s + e^p + \tau \quad (21)$$

The compatibility condition and the boundary conditions are

$$\frac{\partial^2 e}{\partial \eta^2} = 0 \Rightarrow e = f + g\eta \quad (22)$$

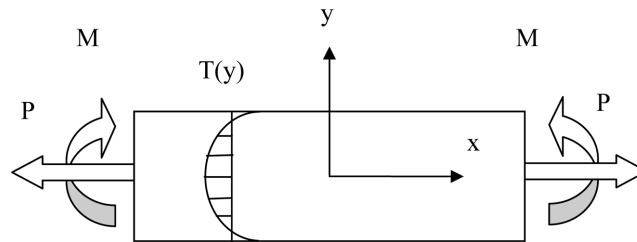


Fig. 2 Applied loads on the beam

$$\int_{-1}^1 s d\eta = \frac{p}{\sigma_y b h} = P \quad (23)$$

$$\int_{-1}^1 s \eta d\eta = \frac{m}{\sigma_y b h^2} = M \quad (24)$$

where b is the beam width and m , M , p and P are the applied moment, dimensionless applied moment, applied axial load and dimensionless axial load, respectively. Substituting Eq. (22) into Eq. (22) for solving s , thus

$$s = f + g\eta - e^p - \tau \quad (25)$$

Using the boundary conditions (23) and (24), the constants of integration f and g are obtained as follows

$$f = \frac{B[M + \int_{-1}^1 (1 - D_p)(e^p + \tau)\eta d\eta] - K[P + \int_{-1}^1 (1 - D_p)(e^p + \tau)d\eta]}{B^2 - AK} \quad (26)$$

$$g = \frac{B[P + \int_{-1}^1 (1 - D_p)(e^p + \tau)d\eta] - A[M + \int_{-1}^1 (1 - D_p)(e^p + \tau)\eta d\eta]}{B^2 - AK} \quad (27)$$

where

$$A = 2 - \int_{-1}^1 D_p d\eta, \quad B = -\int_{-1}^1 D_p \eta d\eta, \quad K = \frac{2}{3} - \int_{-1}^1 D_p \eta^2 d\eta \quad \text{and } D_p \text{ corresponds to the plastic damage.}$$

with the help of the defined dimensionless parameters in Eq. (20), yield function reduces to

$$f(\tilde{\sigma}, X) = \left| \frac{s}{1 - D_p} - x \right| - 1 = 0 \quad (28)$$

3.1 Creep damage formulation

Elasto plastic thermal and mechanical stresses were developed for a damaged beam. In what follows, let us introduce and take into account the effect of creep. Using the strain separation principle, the creep strain can be added to the total strain and so the rate of the normalized stress-strain relation (21) with the help of the compatibility relation (22), is as follows

$$\dot{s} = \dot{f} + \dot{g}\eta \quad (29)$$

with substitution of the above equation in the boundary conditions, two coefficients can be obtained as

$$\dot{f} = \frac{gB' \int_{-1}^1 \dot{D}_f \eta^2 d\eta - (fB' - gK') \int_{-1}^1 \dot{D}_f \eta d\eta - fK' \int_{-1}^1 \dot{D}_f d\eta}{B'^2 - A'K'} \quad (30)$$

$$\dot{g} = \frac{-gA' \int_{-1}^1 \dot{D}_f \eta^2 d\eta + (gB' - fA') \int_{-1}^1 \dot{D}_f \eta d\eta + fB' \int_{-1}^1 \dot{D}_f d\eta}{B'^2 - A'K'} \quad (31)$$

where

$A' = \int_{-1}^1 (1 - D_f) d\eta$, $B' = \int_{-1}^1 (1 - D_f) \eta d\eta$, $K' = \int_{-1}^1 (1 - D_f) \eta^2 d\eta$ and D_f corresponds to the creep damage. The total damage is the sum of the elasto-plastic and creep damage

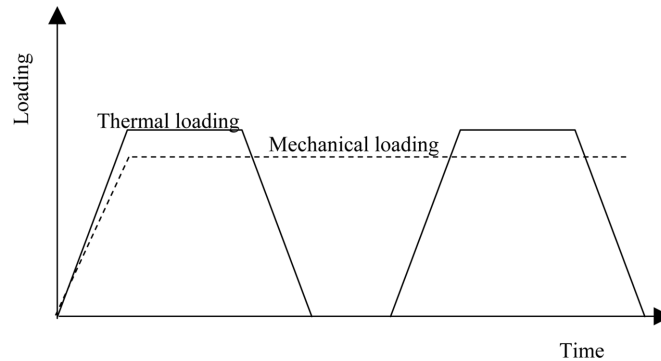


Fig. 3 Description of a loading cycle

$$D = D_p + D_f \quad (32)$$

For the creep evolution, the damage is computed in the cycle by integration Eq. (13) at every time step with the corresponding mean values of A_D and r_D which are temperature dependent.

4. Numerical solution

The necessary equations for the analysis were obtained. A cycle consists four steps: thermal and/or mechanical loading, creep, unloading and creep (Fig. 3). To determine the response of the beam, the first step consists on dividing the beam depth into n layers and then applying loads, with the elastic assumption. Determining the maximum equivalent stress in every depth is carried out in a second step. The plastic boundaries are determined in the third step. Eqs. (25)-(27) give the stress distribution. In order to solve the equations, the following steps were done:

1. The accumulated plastic strain for the first increment of the load in the plastic region is set to zero.
2. Assuming the incremental damage parameter, dD , to be zero, Eqs. (25) and (28) can be solved in order to determine the incremental plastic strain.
3. Calculation of the current value of the incremental damage parameter according to the incremental plastic strain obtained in the last step.
4. Calculation of the total damage parameter.
5. Repeating the procedure from step 2 (with the obtained non zero value of dD) through 4, until the current value of the increment of the equivalent plastic strain converges.
6. Adding the converged value of the increment of current equivalent plastic strain to the accumulated plastic strains.
7. The load is increased one step and the procedure is repeated until the final value of the load is reached.

At creep step time, Eqs. (29)-(31) permit to determine the evolution of stresses and strains. In the unloading step, the mechanical and/or the thermal load is subtracted and the loads in Eqs. (25)-(27) are replaced with negative values. In the final step, creep Eqs. (29)-(31), determine the final strain and the stress values at the end of every cycle. For every cycle, repeating these steps will yield the structure response. The flow chart of the numerical procedure is given in the Fig. 4.

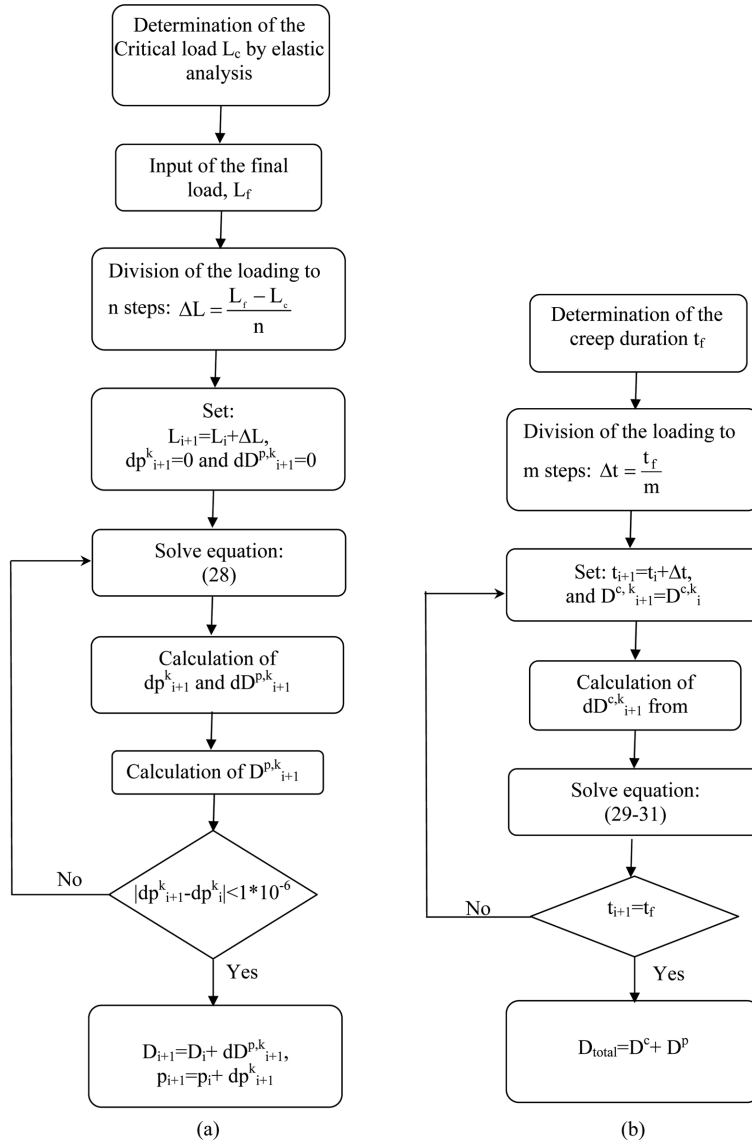


Fig. 4 Flowchart of the stress-strain computations for a) plastic part and b) creep part

5. Results and discussions

Three types of axial, bending, and thermal loads are applied to show their ratcheting or shakedown behavior as the result of cyclic loading. The Non linear kinematic hardening, the continuum ductile plastic and creep damage theory are used in order to obtain the Bree's interaction diagram for two different loadings. For the first case a constant bending moment was applied and a cyclic thermal gradient with parabolic temperature distribution $\tau = \tau_0(\eta^2 - 1/3)$ was added. In the second case the constant bending moment was replaced with a constant axial load.

Table 1 Used material properties

E (GPa)	σ_y (MPa)	C (MPa)	γ	D_c	ε_p^D	ε_p^R	A_D (MPa)	r_D
193	193	896	60	0.24	0.02	0.37	1160	6.5

The beam data are: modulus of elasticity $E=210$ GPa, $C=20$ GPa, and $\gamma=60$. The ductile plastic damage parameters are considered as follows: critical damage parameter, $D_c=0.24$, low limit of damage, $\varepsilon_p^D=0.02$ and upper limit of damage, $\varepsilon_p^R=0.37$. $A_D=1160$ MPa and $r_D=6.5$ are creep damage parameters (Table 1). The damage parameters are temperature dependent. In this research, the average value of the model parameters between maximum and minimum temperatures was used.

The interaction diagram of a beam under mentioned conditions was obtained using the developed numerical program. The applied loads are a mechanical load superposed with a cyclic temperature gradient. In each mechanical and thermal loads combination, the temperature gradient is incrementally increased and decreased while mechanical load is constant throughout the cycles.

In order to obtain the Bree's diagram, first, the mechanical load was applied. The mechanical loads (axial load and bending moment) were considered less than critical load, so the applied stresses and strains can be obtained from the elastic analysis. The thermal loading consists of varying temperature distribution across the beam height and increasing from zero. When the temperature gradient attains its maximum, thermal loading stays constant during creep part. Then the temperature gradient decreased until zero gradient reached. At this point, a thermal stress cycle is completed. Up to 80 cycles are applied to obtain a steady cyclic state for different combination of mechanical and thermal loadings. Using these results, the boundary between shakedown and ratchetting regions were obtained.

For example, Figs. 5(a) and (b) shows the behavior of a beam under the constant mechanical axial load $P=0.7$ and the cyclic temperature gradient. A thermal load with parabolic temperature distribution $\tau = \tau_0(\eta^2 - 1/3)$ and τ_0 parameter between $\tau_0 = -3.2$ and 3.2 , was applied. The average axial strain is not zero and the ratcheting phenomenon appeared.

Reducing the maximum temperature, ratchetting behavior changes to elastic shakedown behavior. Figs. 5(c) and (d) shows the stress - plastic strain evolution under the constant mechanical axial load $P=0.6$ together with and the maximum temperature cyclic load $\tau_0 = 2.5$. Instead of the constant axial load, the constant bending moment was applied and the same behavior was obtained. In the shakedown behavior (Fig. 5a) the damage parameter, D , is constant and does not increase (Fig. 6a) but in the ratchetting case, the damage parameter increases rapidly (Fig. 6b). When $D=D_c$ the failure is reached.

Fig. 7 is the interaction diagram for the thermal load parameter versus bending moment parameter. Replacing the bending moment with the axial load, the same regions as in Fig. 8 have been seen in this figure and the same assumptions are used to evaluate the limits of these three regions. The results show a considerable reduction of shakedown loads due to the combination of creep and plastic damage compared to the undamaged or ductile damage behavior, particularly where the mechanical loads are dominant.

6. Conclusions

Stresses are categorized as primary, secondary, or peak. Primary stresses are a concern for

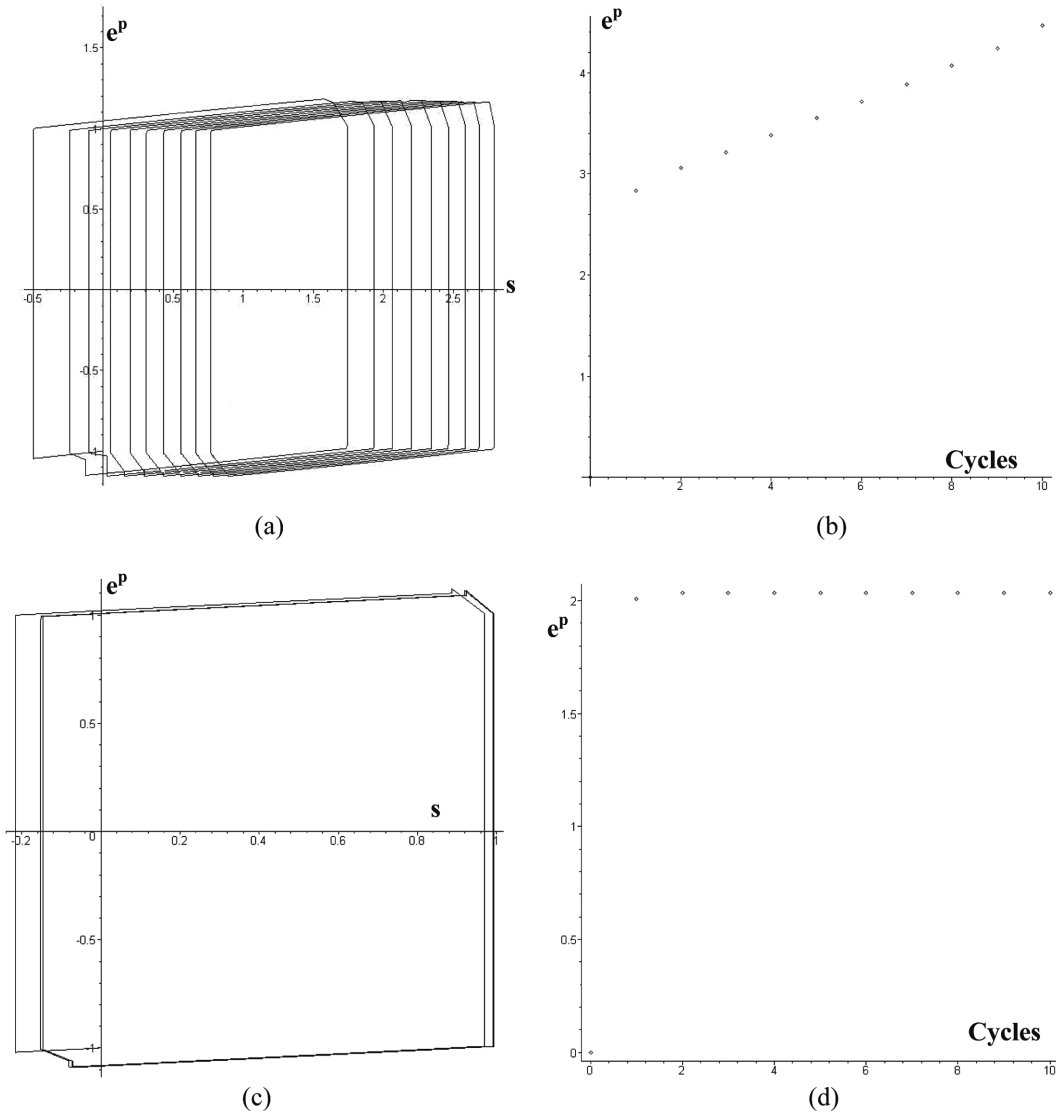


Fig. 5 a) stress-plastic strain and b) strain evolution in each cycle for $P=0.7$ and $\tau_0=3.2$ and c) stress-plastic strain and d) strain evolution in each cycle $P=0.6$ and $\tau_0=2.5$

deformation, burst, or collapse. Secondary stresses are limited to require shakedown to elastic action to ensure the applicability of the fatigue evaluation. Peak stresses are a concern for fatigue. Primary stresses are required for equilibrium with an internal or external applied mechanical load. Axial load and bending moment are mechanical loads and cause primary stress. Thermal expansion through-beam depth temperature distribution is not a mechanical load and, therefore produces a secondary stress. A secondary stress is displacement controlled and is self-limiting.

In this paper, a numerical iterative method is proposed which is quite able and efficient to handle the cyclic loading analysis of structures with damage problems. Using this method, the elastoplastic cyclic loading of a beam behavior was obtained. The non linear kinematic hardening model coupled

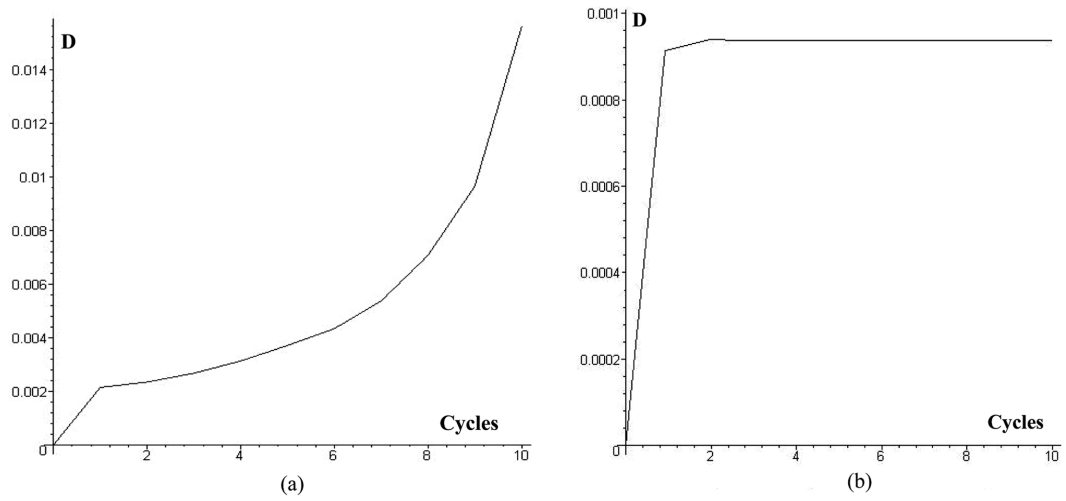


Fig. 6 Damage evolution during cycles for a) $P=0.7$ and $\tau_0=3.2$, b) $P=0.6$ and $\tau_0=2.5$

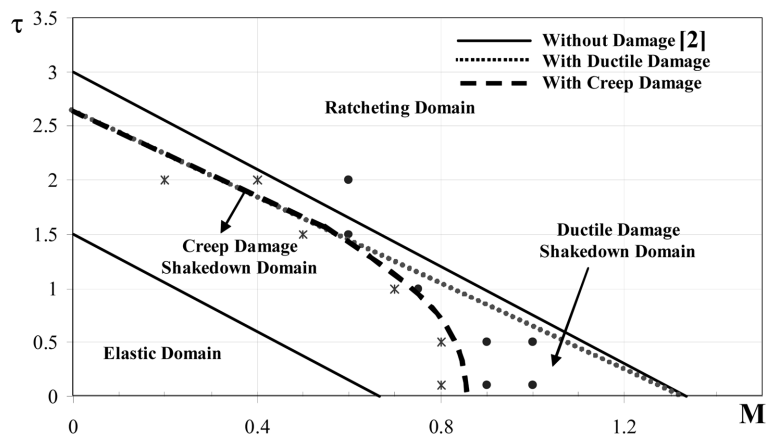


Fig. 7 Interaction diagram for thermal load parameter versus bending moment load

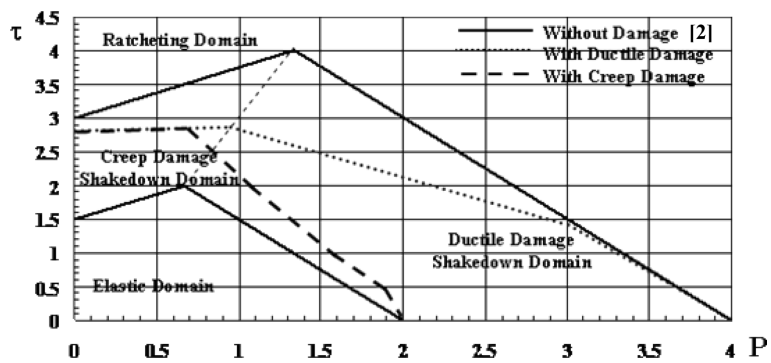


Fig. 8 Interaction diagram for thermal load parameter versus axial load

with creep and ductile damage model is employed to evaluate the results of cyclic loadings.

Up to the knowledge of the author, the damage phenomena was considered in the Bree's interaction diagram for the first time and it was shown that the reduction of the shakedown limit was more important when secondary stresses diminished and in the same time the primary stresses increased.

The proposed method is simple and allows the cyclic behavior of damaged structures to be studied. However, as ductile and creep damage is often induced by large plastic strains, in future studies it will be necessary to take the influence of large plastic strains on shakedown into account.

Nomenclatures

A_D	Material Parameter
b	Beam width
C	Non linear kinematic hardening model's constant
D	Damage parameter
D_c	Interatomic decoherence damage parameter
e	Non dimensional total strain
e^p	Non dimensional plastic strain
E	Elastic modulus
\tilde{E}	Effective elastic modulus
h	Beam height
m	Applied moment
M	Non dimensional applied moment
\dot{p}	Incremental accumulated plastic strain
p	Applied axial load
P	Non dimensional applied axial load
r_D	Material Parameter
s	Non dimensional applied axial stress
S	Virgin surface
\tilde{S}	Resistant effective surface
T	Temperature
X	Back stress
X'	Deviatoric back stress
Y	Associate thermodynamics damage variable
α	Expansion coefficient
γ	Non linear kinematic hardening material constant
η	Non dimensional depth
ε_p	Plastic strain
ε_T	Thermal strain
$\varepsilon_p^D, \varepsilon_p^R$	Strain damage constants
σ	Theoretical axial stress
$\tilde{\sigma}$	Effective stress
σ'	Deviatoric stress
σ_H	Hydrostatic stress
σ_{eq}	Equivalent Von-Mises stress
σ_y	Yield stress
τ	Non dimensional thermal strain
ν	Poisson's coefficient

References

- ASME (1998), III, Division I, Subsection NH, App. T.
- Bree, J. (1967), "Elastic-plastic behavior of thin tubes subjected to internal pressure and intermittent high-heat fluxes with application to fast-nuclear-reactor fuel elements", *J. Strain Anal.*, **2**, 226-238.
- Chaboche, J.L. and Lemaitre, J. (1990), *Mech. Mater.*, Cambridge University Press.
- Chandrakanth, S. and Pandey, P.C. (1995), "An isotropic damage model for ductile material", *Eng. Fract. Mech.*, **50**(4), 457-465.
- Coffin, L.F. (1954), "A study of cyclic thermal stress in a ductile metal", *Trans. ASME*, **76**, 931-950.
- Coffin, L.F. (1976), "The concept of frequency separation methods in life prediction for time dependent fatigue", *ASME Symp. on Creep Fatigue Interaction*, 346-363.
- Desmorat, R., Kane, A., M. Seyed, and Sermage, J.P. (2007), "Two scale damage model and related numerical issues for thermomechanical high cycle fatigue", *Eur. J. Mech. A/Solids*, **26**, 909-935.
- Eslami, M.R. and Mahbadi, H. (2002), "Cyclic loading of beams based on the Prager and Frederick–Armstrong kinematic hardening models", *Int. J. Mech. Sci.*, **44**, 859-879.
- Krajcinovic, D. (1979), "Distributed damage theory of beams in pure bending", *J. Appl. Mech. - T. ASME*, **46**, 592-596.
- Lemaitre, J. (1985), "A continuous damage mechanics model for ductile fracture", *J. Eng. Mater. - T. ASME*, **107**, 83-89.
- Lemaitre, J. (1992), *A Course on Damage Mechanics*, Springer-Verlag, Berlin.
- Lemaitre, J. and Chaboche, J.L. (1974), "A non-linear model of creep-fatigue damage accumulation and interaction", *IUTAM Symposium*, Göthenburg, Sweden, 291-300.
- Lemaitre, J. and Desmorat, R. (2005), *Engineering Damage Mechanics*, Springer-Verlag, Berlin.
- Lemaitre, J.L. (1984), "How to use damage mechanics", *Nuclear Eng. Design*, **80**, 233-245.
- Mahbadi, H., Gowhari, A.R., and Eslami, M.R. (2004), "Elastic–plastic–creep cyclic loading of beams using the Prager kinematic hardening model", *J. Strain Anal.*, **39**, 127-136.
- Manson, S.S. (1954), "Behavior of materials under conditions of thermal stress", *NACA Technical Note*, TN-2933.
- Manson, S.S. (1971), "Creep fatigue analysis by strain range partitioning", *ASME Symp. on Design for Elevated Temperature*, ASME, San Francisco.
- O'Donnell, W.J. and Porowski, J.S. (1981), "Biaxial model for bounding creep ratcheting", *ORNL Report ORNL/Sub7322/2*, ORNL, Oak Ridge, TN.
- Sermage, J.P., Lemaitre, J., and R. (2000), "Desmorat, Multiaxial creep-fatigue under anisothermal conditions", *Fatig. Fract. Eng. M.*, **23**, 241-252.
- Shi, G and Voyiadjis, G.Z. (1993), "A computational model for fe ductile plastic damage analysis of plate bending", *J. Appl. Mech.*, **60**, 749-758.
- Taira, S. (1962), *Creep in Structures*, Academic Press.